

Polarization of top quark as a probe of its chromomagnetic and chromoelectric couplings in tW production at the Large Hadron Collider

Saurabh D. Rindani¹, Pankaj Sharma² and Anthony W. Thomas²

¹ *Theoretical Physics Division, Physical Research Laboratory,
Navrangpura, Ahmedabad 380 009, India*

² *Center of Excellence in Particle Physics (CoEPP),
University of Adelaide, Adelaide, Australia*

Abstract

We study the sensitivity of the Large Hadron Collider (LHC) to top quark chromomagnetic (CMDM) and chromoelectric (CEDM) dipole moments and Wtb effective couplings in single-top production in association with a W^- boson, followed by semileptonic decay of the top. The Wt single-top production mode helps to isolate the anomalous ttg and Wtb couplings, in contrast to top-pair production and other single-top production modes, where other new-physics effects can also contribute. We calculate the top polarization and the effects of these anomalous couplings on it at two centre-of-mass (cm) energies, 8 TeV and 14 TeV. As a measure of top polarization, we look at decay-lepton angular distributions in the laboratory frame, without requiring reconstruction of the rest frame of the top, and study the effect of the anomalous couplings on these distributions. We construct certain asymmetries to study the sensitivity of these distributions to top-quark couplings. We determine individual limits on the dominant couplings, viz., the real part of the CMDM $\text{Re}\rho_2$, the imaginary part of the CEDM $\text{Im}\rho_3$, and the real part of the tensor Wtb coupling $\text{Re}f_{2R}$, which may be obtained by utilizing these asymmetries at the LHC. We also obtain simultaneous limits on pairs of these couplings taking two couplings to be non-zero at a time.

1 Introduction

The top quark is the heaviest fundamental particle discovered so far with mass $m_t = 173.2 \pm 0.9$ GeV [1]. Mainly for this reason, it is considered to be one of the most likely places where new physics might be discovered. While enough information about the top quark is already available, showing consistency with SM expectations, future runs at the Large Hadron Collider (LHC) will enable a more precise determination of its properties. In particular, if new physics contributions to the interactions of the top quark are written in terms of anomalous couplings, it will be possible to constrain these couplings quantitatively. The experimental study involves the measurement of production cross sections, kinematic distributions in production and decay characteristics. With the availability of high statistics, it should also be possible to investigate finer details like top polarization, which can give more information about its interactions.

Because of its large mass, the top-quark life time is very short and it decays spontaneously before any non-perturbative QCD effects can force it into a bound state. Thus, its spin information is preserved in terms of the differential distribution of its decay products. So by studying the kinematical distributions of top decay products, it is, in principle, possible to measure the top polarization in any top production process.

Top polarization and its usefulness in the study of new physics scenarios has been extensively treated in the literature. For reviews see [5, 6]. Some recent papers in the context of hadron colliders are [7, 8, 9, 10, 11, 12, 13, 14, 15, 16]. For example, in Ref. [8], it was shown in the context of an extra Z model how decay-lepton asymmetries in the lab. frame could be used to measure top polarization. Ref. [9, 10] studied the top polarization in associated single-top production with charged Higgs in two Higgs doublet model (2HDM) and the minimal supersymmetric extension of standard model (MSSM). The effect of anomalous Wtb couplings on top polarization in single-top production in association with W has been studied, without [11] and with CP violation [13]. Constraining top-quark chromomagnetic (CMDM) and chromoelectric (CEDM) dipole couplings using top polarization observables in the context of Tevatron and LHC has been studied in [7, 14]. Ref. [15] discusses the use of top polarization to determine the charged-Higgs mass and to distinguish various 2HDMs in associated tH^- production at the LHC. Refs. [16] suggest utilizing top polarization as a probe of models for the top forward-backward asymmetry observed at the Tevatron.

At the LHC, top quarks are produced mainly via two independent mechanisms. The dominant one is $t\bar{t}$ pair production which occurs through gluon fusion and quark-antiquark annihilation. The second mechanism is single top production [17, 18, 19, 20, 21, 22, 23, 24, 25, 26, 27, 28, 29, 30, 31, 32]. Since the latter proceeds via weak interaction, top quarks tend to have large polarization [23, 24]. At LHC energies, single-top quark events in the SM are produced in three different modes: a) the t -channel ($bq \rightarrow tq'$), b) the s -channel ($q\bar{q}' \rightarrow t\bar{b}$) and c) the Wt production process ($bg \rightarrow tW^-$) [21]. These three modes are completely different kinematically and can be separated from one another. Of these, the t -channel [28, 29, 30] and the Wt [31, 32] processes have been observed at the LHC. Despite having smaller cross section than top pair production, single-top production is an important tool to study effects which may not be accessible in top

pair production. For example, single-top production allows an independent measurement of the CKM matrix element V_{tb} . Also, unlike top-pair production, single-top production gives rise to large top-quark polarization. Top polarization has indeed been measured at the LHC [35] in the t -channel process, and found to be consistent with the SM prediction, within somewhat large errors.

Run 2 has recently commenced with center of mass (cm) energy of 13 TeV. The LHC is expected to run at this energy for about a year collecting around 30 fb^{-1} of integrated luminosity. The next run of the LHC will be a high-luminosity run with a slightly increased cm energy of 14 TeV. This run is expected to acquire a tremendous amount of data (around 3000 fb^{-1}). In this work, we focus on the 8 and 14 TeV runs of the LHC and present all the results for them. The priorities at the LHC in the analysis of these large data sets would be to first determine accurately the total and differential cross sections for the dominant top-pair production process, followed by those for single-top processes. This will help to constrain anomalous couplings contributing to the cross sections for these processes. However, there are competing contributions from several sources. In such a scenario, closer detailed examination of top polarization and the consequent decay distributions would be helpful in isolating those sources.

In this work, we study Wt production at the LHC in the presence of anomalous gluon couplings to top quarks. In particular, we examine the possibility of using top polarization and other angular observables, constructed from top decay products in the laboratory frame, to measure these couplings. Our main emphasis will be to show how these laboratory-frame observables can be used to probe the anomalous couplings. We calculate our observables at the LHC with centre-of-mass (cm) energies of 8 TeV (LHC8) and 14 TeV (LHC14). We also study the sensitivities of these observables to anomalous top quark couplings including statistical uncertainties with integrated luminosities 20 fb^{-1} at LHC8 and 30 fb^{-1} for the case of LHC14. Our results will go through with little change for the present run of the LHC at 13 TeV for a similar luminosity.

Top quark couplings to a gluon can be defined in a general way as

$$\Gamma^\mu = \rho_1 \gamma^\mu + \frac{2i}{m_t} \sigma^{\mu\nu} (\rho_2 + i\rho_3 \gamma_5) q_\nu, \quad (1)$$

where ρ_2 and ρ_3 are top quark CMDM and CEDM form factors and m_t is the mass of top quark. Of these, the ρ_2 term is CP even, whereas the ρ_3 term is CP odd. In the SM, both ρ_2 and ρ_3 are zero at tree level. Top CMDM and CEDM couplings, which we study here, could arise in the SM or from new interactions at loop level. While the CP-conserving CMDM coupling can arise in the SM at one-loop [36], the CP-violating CEDM coupling can only be generated at 3-loop level in the SM [37]. These couplings have been calculated at one-loop level in various new physics models such as MSSM [38], 2HDM [39, 40], Little Higgs model [41] and in models with unparticles [42].

Top chromomagnetic and chromoelectric dipole moments have been examined in the past in the context of single-top production [43, 44, 45], top-pair production [14, 46, 47, 48, 49, 50, 51, 52, 53], and top-pair plus jet production [54] at hadron colliders. Cheung [55] has used spin correlations in top-pair production at hadron colliders to probe top CMDM and CEDM. CP violation in top-pair production at hadron colliders including top CEDM couplings is studied in

[56].

Apart from having a direct effect on top-pair production at hadron colliders, top CMDM and CEDM couplings can have an indirect effect and modify the decay rate of $b \rightarrow s\gamma$ at loop level [58, 59]. Using the measured branching ratio $\text{Br}(b \rightarrow s\gamma)$ [59], tight bounds on the top CMDM, ρ_2 , were extracted, viz., $0.03 < \rho_2 < 0.01$.

Any new physics in which new couplings to top are chiral can influence top polarization. The measurement of top polarization is thus an important tool to study new physics in single-top production. However, top polarization can only be measured through the distributions of its decay products. Hence, any new physics in top decay may contaminate the measurement of top polarization, and therefore of the new physics contribution in top production. Assuming only SM particles, any new physics in top decay can be parametrized in terms of anomalous tbW couplings as

$$\Gamma^\mu = \frac{-ig}{\sqrt{2}} V_{tb} \left[\gamma^\mu (f_{1L} P_L + f_{1R} P_R) + \frac{i\sigma^{\mu\nu}}{m_W} (p_t - p_b)_\nu (f_{2L} P_L + f_{2R} P_R) \right] \quad (2)$$

where the in SM $f_{1L} = 1$ and $f_{1R} = f_{2L} = f_{2R} = 0$. Under the assumptions that (i) anomalous tbW couplings are small, (ii) the top is on-shell and (iii) $t \rightarrow bW^+$ is the only decay channel, it was shown in Refs. [60] that the charged-lepton angular distributions are independent of the anomalous tbW couplings, a result proven earlier under less general circumstances [61]. Thus, one can say that the charged-lepton angular distributions are clean and uncontaminated probes of top polarization and thus of any new physics responsible for top production. We would make use of this property and use charged-lepton angular distributions as a probe of top polarization. However, to the extent that the production process also involves tbW couplings, anomalous tbW couplings will enter our considerations, and we will also look at possible limits that could be placed on them.

The rest of the paper is organized as follows. In the next section we introduce the formalism and the framework of our work. In Section 3 we discuss the process of Wt mode of single top production at the the LHC and present our results for the observables like top polarization, charged-lepton angular distributions and the lepton azimuthal asymmetry. Section 4 deals with the statistical sensitivity of our observables to the anomalous couplings. The conclusions are given in Section 5. The Appendix lists the production spin density matrix elements at the parton level including the contributions of anomalous top couplings.

2 Framework and analytical results

The main aim of this work is to study the effect of anomalous top-gluon couplings on the top quark polarization and other angular observables in Wt production at the LHC. For the calculation of final charged-lepton distributions, we use spin-density matrix formalism. We use the narrow-width approximation (NWA)

$$\left| \frac{1}{p^2 - m^2 + im\Gamma} \right|^2 \sim \frac{\pi}{m\Gamma} \delta(p^2 - m^2) \quad (3)$$

to factor the matrix amplitude squared into production and decay parts as

$$|\overline{\mathcal{M}}|^2 = \frac{\pi\delta(p_t^2 - m_t^2)}{\Gamma_t m_t} \sum_{\lambda, \lambda'} \rho(\lambda, \lambda') \Gamma(\lambda, \lambda'), \quad (4)$$

where $\rho(\lambda, \lambda')$ and $\Gamma(\lambda, \lambda')$ are the 2×2 top production and decay spin density matrices and $\lambda, \lambda' = \pm 1$ denotes the sign of the top helicity.

We obtain analytical expressions for the spin density matrix for Wt production including anomalous couplings. Use is made of the analytic manipulation program FORM [62]. We find that at linear order, Ref_{2R} , $\text{Re}\rho_2$ and $\text{Im}\rho_3$ give significant contributions to the production density matrix, whereas contributions from all other couplings are proportional to the mass of b quark (which we neglect consistently) and hence vanish in the limit of zero bottom mass. To second order in anomalous couplings, other anomalous couplings do contribute, but we focus on Ref_{2R} , $\text{Re}\rho_2$ and $\text{Im}\rho_3$, since their contributions, arising at linear order, are dominant. Expressions for the spin density matrix elements $\rho(\pm, \pm)$ and $\rho(\pm, \mp)$, where \pm are the signs of the top-quark helicity, for Wt production including the contributions of $\text{Re}\rho_2$ and $\text{Im}\rho_3$ are given in the Appendix. The expressions for production and top-decay spin-density matrices, for anomalous Wtb couplings, have been evaluated in Ref. [11].

Using the NWA and spin-density matrix formalism for top production and its decay, we write the partial cross section in the parton cm of frame as

$$d\sigma = \frac{1}{32(2\pi)^4 \Gamma_t m_t} \int \left[\sum_{\lambda, \lambda'} \frac{d\sigma(\lambda, \lambda')}{d\cos\theta_t} \left(\frac{\langle \Gamma(\lambda, \lambda') \rangle}{p_t \cdot p_\ell} \right) \right] \times d\cos\theta_t d\cos\theta_\ell d\phi_\ell E_\ell dE_\ell dp_W^2, \quad (5)$$

where the b -quark energy integral is replaced by an integral over the invariant mass p_W^2 of the W boson, its polar-angle integral is carried out using the Dirac delta function of Eq. (3), and the average over its azimuthal angle is denoted by the angular brackets. Integrating over the lepton energy, with limits given by $m_W^2 < 2(p_t \cdot p_\ell) < m_t^2$, the analytical expression for the differential cross section in the parton cm frame is given as

$$\frac{d\sigma}{d\cos\theta_t d\cos\theta_\ell d\phi_\ell} = \frac{1}{32 \Gamma_t m_t} \frac{1}{(2\pi)^4} \int \left[\sum_{\lambda, \lambda'} \frac{d\sigma^{\lambda\lambda'}}{d\cos\theta_t} g^4 \mathcal{A}^{\lambda\lambda'} \right] |\Delta(p_W^2)|^2 dp_W^2, \quad (6)$$

where

$$\mathcal{A}^{\pm\pm} = \frac{m_t^6}{24(1 - \beta_t \cos\theta_{t\ell})^3 E_t^2} \left[(1 - r^2)^2 (1 \pm \cos\theta_{t\ell}) (1 \mp \beta_t) (1 + 2r^2) \right], \quad (7)$$

$$\mathcal{A}^{\pm\mp} = \frac{m_t^7}{24(1 - \beta_t \cos\theta_{t\ell})^3 E_t^3} \sin\theta_{t\ell} e^{\pm i\phi_\ell} \left[(1 - r^2)^2 (1 + 2r^2) \right]. \quad (8)$$

Here $r = m_W/m_t$ and $\cos\theta_{t\ell}$ is the angle between the top quark and the charged lepton in top decay in the parton cm frame, given by

$$\cos\theta_{t\ell} = \cos\theta_t \cos\theta_\ell + \sin\theta_t \sin\theta_\ell \cos\phi_\ell, \quad (9)$$

where θ_ℓ and ϕ_ℓ are the lepton polar and azimuthal angles.

3 Single-top production in association with a W boson

The theoretical mechanism for the tW^- mode of single-top production has been studied in detail in Refs. [21, 25, 26]. At the parton level, the tW^- production proceeds through a gluon and a bottom quark each coming from a proton and gets contributions from two diagrams. Feynman diagrams for the process $g(p_g)b(p_b) \rightarrow t(p_t, \lambda_t)W^-$, where $\lambda_t = \pm 1$ represents the top helicity, are shown in Fig. 1. The blobs denote effective tbW and ttg vertices, including anomalous couplings, in the production process.

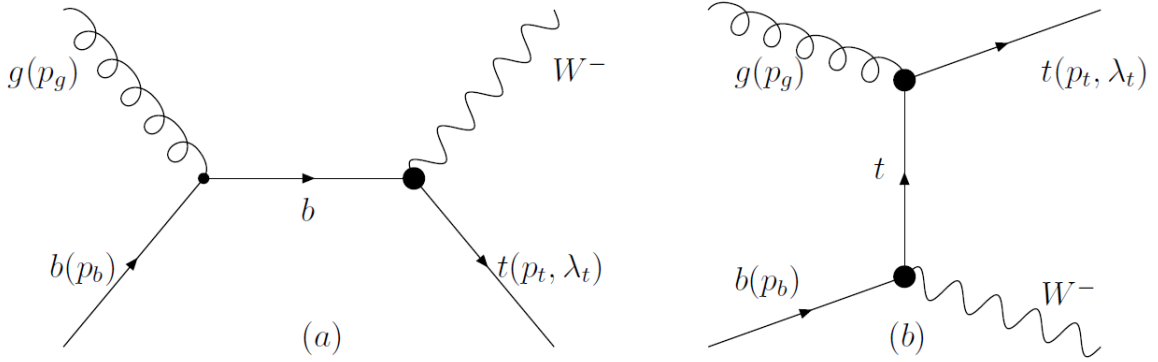


Figure 1: Feynman diagrams for the Wt production process. The blobs here denote the anomalous tbW and ttg couplings.

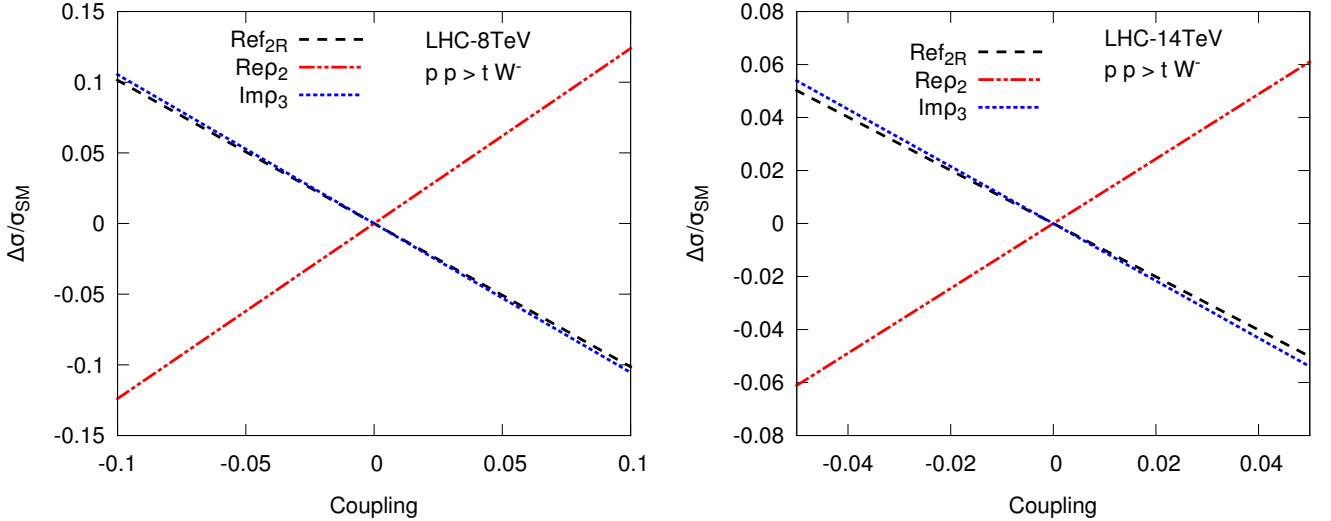


Figure 2: The cross section for tW^- production at the LHC8 (left) and LHC14 (right), as a function of the anomalous tbW and ttg couplings with linear approximation.

For numerical calculations, we use the leading-order parton distribution function (PDF) sets of CTEQ6L [63], with a factorization scale of $m_t = 173.2$ GeV. We also evaluate the strong

coupling at the same scale, $\alpha_s(m_t) = 0.1085$. We make use of the following values of other parameters: $M_W = 80.403$ GeV, the electromagnetic coupling $\alpha_{em}(m_Z) = 1/128$ and $\sin^2 \theta_W = 0.23$. We set $f_{1L} = 1$, $\rho_1 = 1$ and $V_{tb} = 1$ in our calculations. We take only one coupling to be non-zero at a time in the analysis, except in Sec.4.

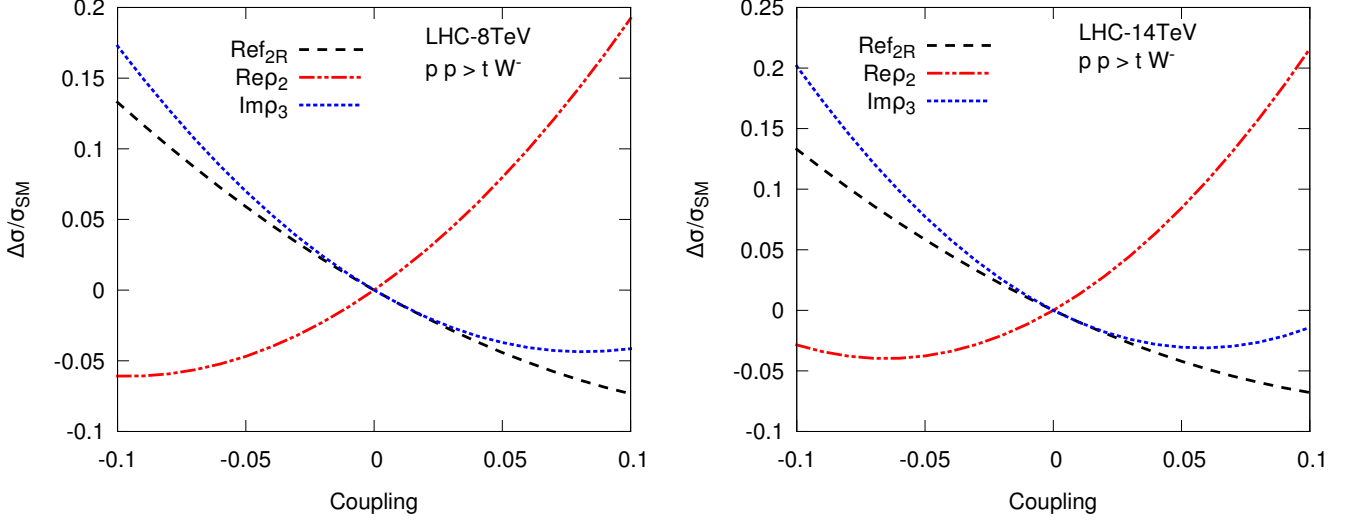


Figure 3: The cross section for tW^- production at the LHC8 (left) and LHC14 (right), as a function of the anomalous tbW and ttg couplings including their contributions at all orders.

After integrating the density matrix given in the Appendix over the phase space, the diagonal elements of this integrated density matrix, which we denote by $\sigma(+, +)$ and $\sigma(-, -)$, are respectively the cross sections for the production of positive and negative helicity tops and $\sigma_{\text{tot}} = \sigma(+, +) + \sigma(-, -)$ is the total cross section. We include the contributions of the anomalous couplings to the cross section at linear order, as well as without that approximation. Since the cross section may receive large radiative corrections at the LHC, we focus on using observables like asymmetries which are ratios of some partial cross sections and are expected to be insensitive to such corrections.

In Fig. 2, we show the relative change in cross section, $\Delta\sigma/\sigma_{SM}$ as a function of various anomalous tbW and ttg couplings when their contributions are taken upto linear order for LHC8 (left) and LHC14 (right), while in Fig. 3 corresponding plots are shown for the full contributions of the anomalous couplings for LHC8 (left) and LHC14(right). From Fig. 3, one can infer that the cross section is very sensitive to negative values of Ref_{2R} and $\text{Im}\rho_3$ and for positive values of $\text{Re}\rho_2$. The linear approximation is seen to be good for values of anomalous couplings Ref_{2R} and $\text{Re}\rho_2$ ranging from -0.05 to 0.05 while for $\text{Im}\rho_3$ it is valid only in the range $[-0.03, 0.03]$.

Recently, the ATLAS and CMS collaborations reported a combination of cross section measurements for tW single top production at $\sqrt{s} = 8$ TeV with integrated luminosities of 20.3 fb^{-1} and 12.2 fb^{-1} , respectively, to be $25.0 \pm 4.7 \text{ pb}$ [34], in agreement with the SM prediction. Using the result of ref. [34] which provides a combined value based upon the cross section measurements from ATLAS and CMS with experimental error, we determine that the fractional change in cross section, at the level of 1σ , constrains the allowed range for $\text{Re}\rho_2$ at $[-0.3, +0.1]$ and

that for $\text{Im}\rho_3$ at $[-0.1, +0.3]$. The limits can be improved at 14 TeV only with much larger integrated luminosity. Ref. [44] estimates that cross section measurement can give constraints on $\text{Re}\rho_2$ and $\text{Im}\rho_3$ of the order of ± 0.01 and ± 0.02 at the LHC14, assuming 5% uncertainty in the measurement. The SM cross section, as also the cross section including anomalous couplings used for the determination of these constraints, are from our computation at the leading order. However, since we consider a fractional change in the cross section to derive our limits, it would be expected to be stable to higher-order corrections and also other uncertainties like PDF and scale uncertainties.

3.1 Top angular distribution

The angular distribution of the top quark would be modified by anomalous couplings. Since the top quark is produced in a $2 \rightarrow 2$ process, its azimuthal distribution is flat. We can study its polar distribution with the polar angle defined with respect to either of the beam directions as the z axis. We find that the polar distribution is sensitive to anomalous tbW couplings.

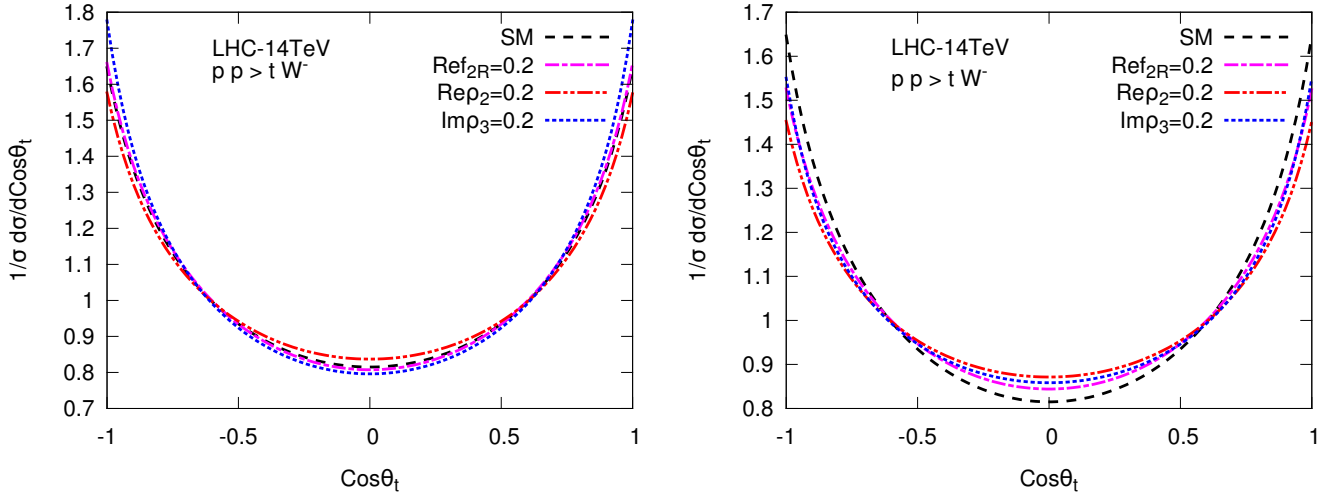


Figure 4: The top polar angular distributions for tW^- production at the LHC14 for different anomalous tbW and ttg couplings with linear approximation (left) and without that approximation (right).

The normalized polar distribution is plotted in Fig. 4 for LHC8 and LHC14. As can be seen from Fig. 4, the curves for the polar distributions for the SM and for the anomalous couplings of magnitude 0.2 are separated from each other. As the colliding beams are identical in the case for LHC, the top polar distribution has no forward-backward asymmetry. However, we can define an asymmetry utilizing the polar distributions of the top quark as

$$\mathcal{A}_\theta^t = \frac{\sigma(|z| > 0.5) - \sigma(|z| < 0.5)}{\sigma(|z| > 0.5) + \sigma(|z| < 0.5)} \quad (10)$$

where z is $\cos\theta_t$. We plot this asymmetry as a function of anomalous tbW and ttg couplings for LHC8 and LHC14 in Fig. 5.

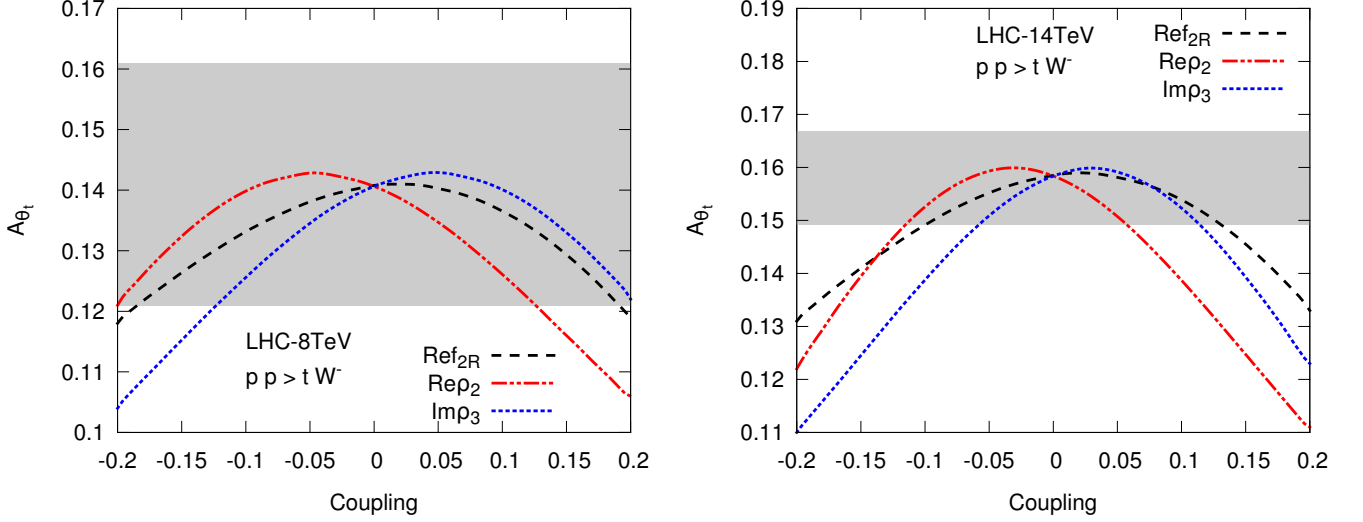


Figure 5: The top polar asymmetries for tW^- production at the LHC8 (left) and LHC14 (right), as a function of anomalous tbW and ttg couplings. The grey band corresponds to the top polar asymmetry predicted in the SM with a 1σ error interval.

The asymmetry \mathcal{A}_θ^t requires accurate determination of the top direction in the lab frame and a quantitative estimate of its sensitivity to anomalous couplings needs details of the efficiency of reconstruction of the direction. We do not study this asymmetry any further, but proceed to a discussion of top polarization.

3.2 Top polarization

$$P_t = \frac{\sigma(+,+) - \sigma(-,-)}{\sigma(+,+) + \sigma(-,-)}. \quad (11)$$

This polarization is shown in Fig. 6 as a function of the anomalous couplings in the linear approximation for LHC8 and LHC14. In Fig. 7 we show the top polarization when full contributions of the couplings have been included. As compared to the SM value of -0.26 for $\sqrt{s} = 14$ TeV, the degree of longitudinal top polarization varies from -0.18 to -0.28 for Ref_{2R} and -0.27 to -0.12 for Rep_2 varied over the range -0.1 to $+0.1$, while it varies from -0.16 to -0.26 for the same range of Imp_3 and is almost symmetric about $\text{Imp}_3 = 0$, which signifies a very small contribution at linear order for Imp_3 .

We notice that, just as for the total cross section, P_t is more sensitive to negative values of Ref_{2R} while for Rep_2 it is more sensitive to positive values of the coupling. Thus P_t will be a very good probe of Ref_{2R} , Rep_2 and Imp_3 if it can be measured at the LHC. However, the standard measurement of P_t requires reconstruction of the top rest frame, which is a difficult task, and would entail a reduction in efficiency. We will therefore investigate lab frame decay distributions for the measurement of the anomalous couplings.

All the quantities considered so far, viz., the total cross section, and the top polarization, can only be measured using information from the decay of the top. Both the polar distribution and

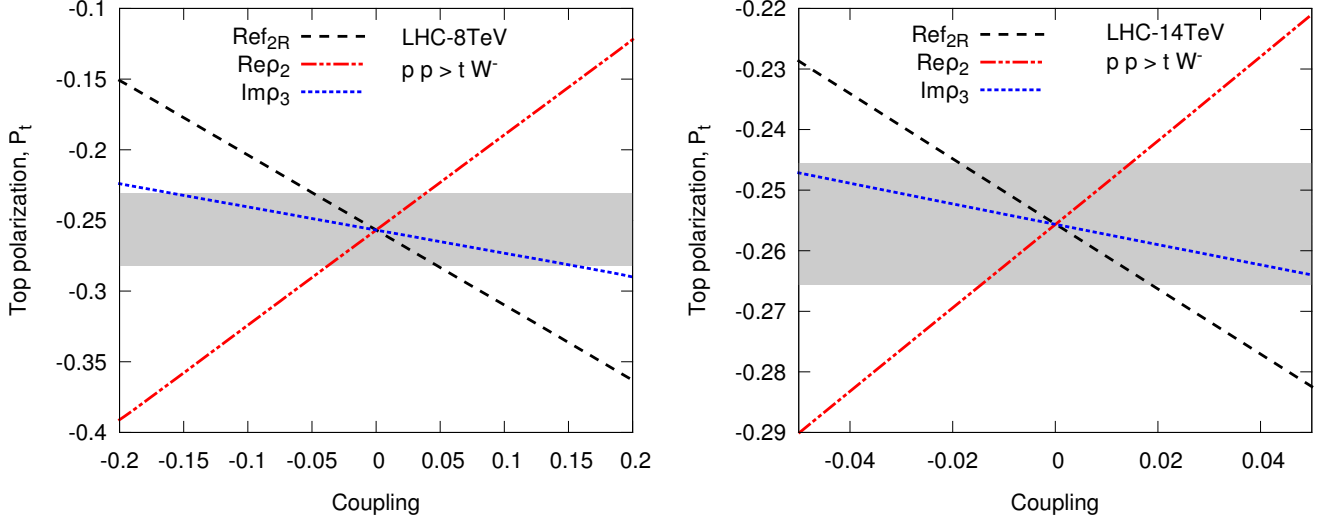


Figure 6: The top polarization for tW^- production at the LHC8 (left) and LHC14 (right) as a function of the anomalous tbW and ttg couplings. The grey band corresponds to the top polarization predicted in the SM with a 1σ error interval.

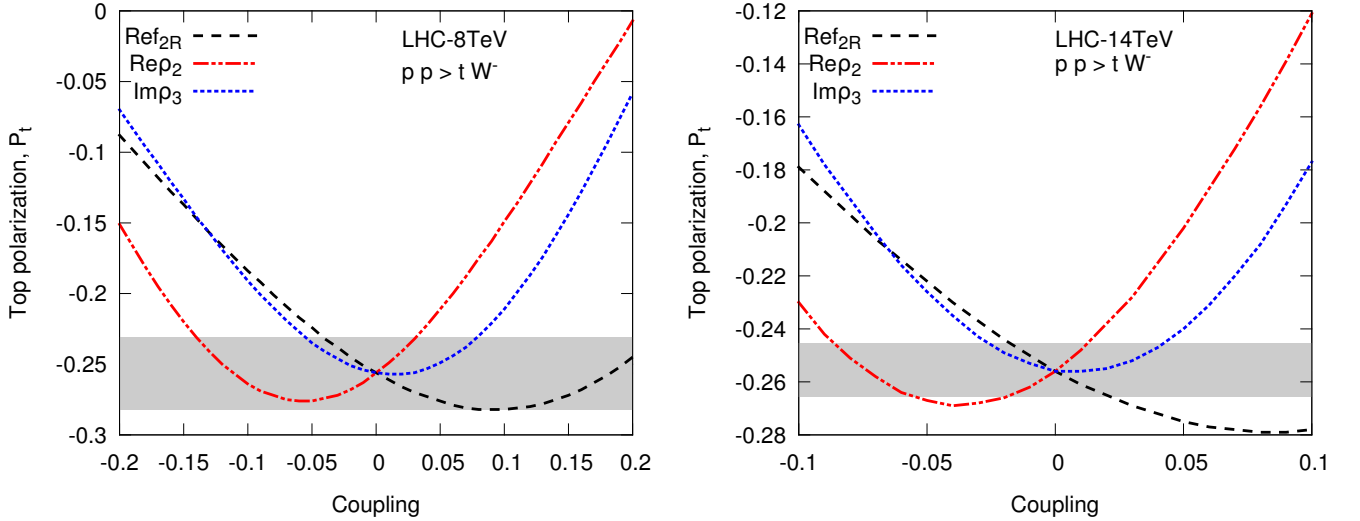


Figure 7: The top polarization for tW^- production at the LHC8 (left) and LHC14 (right) as a function of anomalous tbW and ttg couplings. The grey band corresponds to the top polarization predicted in the SM with a 1σ error interval.

the top polarization would play a role in determining the distributions of the decay products. Our main aim is to devise observables in single-top production which can be measured in the lab frame and give a good estimate of top polarization and hence probe anomalous ttg couplings. We proceed to construct such observables from the kinematic variables of the charged lepton produced in the decay of the top.

3.3 Angular distributions of the charged lepton

Top polarization can be determined through the angular distribution of its decay products. In the SM, the dominant decay mode is $t \rightarrow bW^+$, with a branching ratio (BR) of 0.998, with the W^+ subsequently decaying to $\ell^+\nu_\ell$ (semileptonic decay, BR 1/9 for each lepton) or $u\bar{d}$, $c\bar{s}$ (hadronic decay, BR 2/3). The angular distribution of a decay product f for a top-quark ensemble has the form

$$\frac{1}{\Gamma_f} \frac{d\Gamma_f}{d\cos\theta_f} = \frac{1}{2}(1 + \kappa_f P_t \cos\theta_f). \quad (12)$$

Here θ_f is the angle between the momentum of fermion f and the top spin vector in the top rest frame and P_t (defined in Eq. (11)) is the degree of polarization of the top-quark ensemble. Γ_f is the partial decay width and κ_f is the spin analyzing power of f . Obviously, a larger κ_f makes f a more sensitive probe of the top spin. The charged lepton and the d quark are the best spin analyzers with $\kappa_{\ell^+} = \kappa_{\bar{d}} = 1$, while $\kappa_{\nu_\ell} = \kappa_u = -0.30$ and $\kappa_b = -\kappa_{W^+} = -0.39$, all κ values being at tree level [5]. Thus the ℓ^+ or d have the largest probability of being emitted in the direction of the top spin and the least probability in the direction opposite to the spin. Since at the LHC, the lepton energy and momentum can be measured with high precision, we focus on leptonic decays of the top.

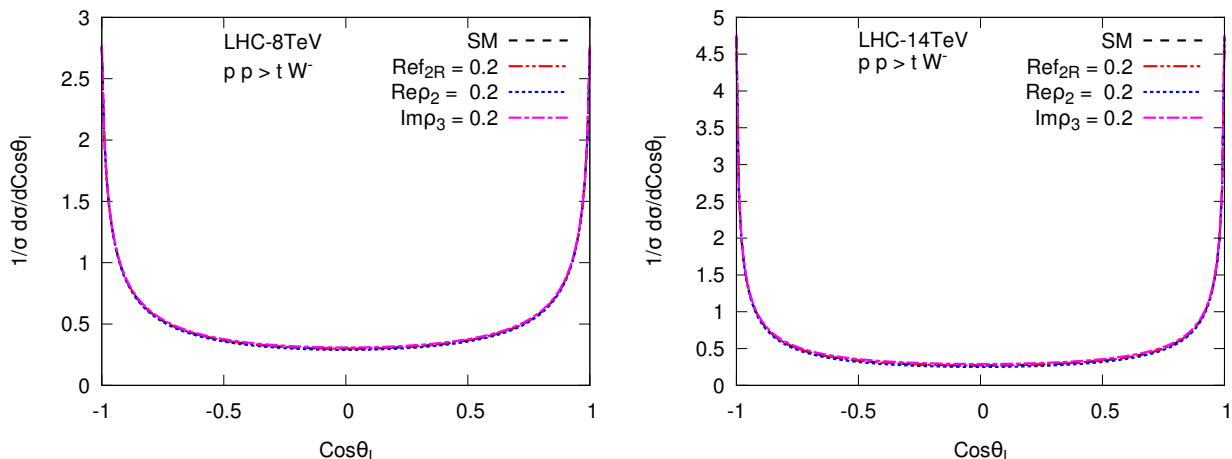


Figure 8: The normalized polar-angle distribution of the charged lepton in associated- Wt single-top production at the LHC8 (left) and LHC14 (right) for the SM and with anomalous Wtb and ttg couplings.

To reconstruct the top-rest frame, one needs full information about the top momentum. However, because of the missing neutrino, it is not possible to reconstruct completely and unambiguously the top longitudinal momentum. This incomplete information may lead to large systematic errors. In this work, we focus on laboratory-frame angular distributions of the charged lepton and thus do not require a full determination of the top momentum. In this sense, the observables we construct are more robust against systematic errors. Also, as mentioned earlier and shown in Refs. [60], the charged-lepton angular distribution in the lab frame is independent

of any new physics in top decay and is thus a clean and uncontaminated probe of new physics in top production.

In the lab frame, we define the lepton polar angle w.r.t. either beam direction as the z axis and the azimuthal angle with respect to the top-production plane chosen, as the x - z plane, with the convention that the x component of the top momentum is positive. At the LHC, which is a symmetric collider, it is not possible to define a positive sense for the z axis. Hence the lepton angular distribution is symmetric under interchange of θ_ℓ and $\pi - \theta_\ell$ as well as of ϕ_ℓ and $2\pi - \phi_\ell$.

We first look at the polar-angle distribution of the charged lepton and the effect on it of anomalous Wtb and ttg couplings. As can be seen from Fig. 8, where we plot the polar-angle distribution for LHC8 and LHC14, the normalized distributions are insensitive to anomalous ttg couplings. The sensitivity of polar-angle distributions on the anomalous ttg couplings in top-pair production have been studied in detail in Ref. [48, 14] for the Tevatron, LHC7 and LHC14 where they find that the polar distribution of the charged lepton is quite sensitive at the Tevatron to anomalous ttg couplings but much less sensitive at the LHC in pair production of top quarks.

We next look at the contributions of anomalous couplings to the azimuthal distribution of the charged lepton. In Figs. 9 we show the normalized azimuthal distribution of the charged lepton in a linear approximation of the couplings for LHC8 and LHC14 for different values of Ref_{2R} , $\text{Re}\rho_2$ and $\text{Im}\rho_3$, taken non-zero one at a time. We see that the curves for the couplings Ref_{2R} , $\text{Re}\rho_2$ and $\text{Im}\rho_3$ peak near $\phi_\ell = 0$ and $\phi_\ell = 2\pi$. The reason for this is two fold: top polarization and kinematic effect. From Eq. (12), one finds that the decay lepton prefers to be emitted along the top spin direction in the top rest frame, with $\kappa_f = 1$. The corresponding distributions in the parton cm frame are given by Eq. (6). The rest frame forward (backward) peak corresponds to a peak for $\cos\theta_{t\ell} = \pm 1$. This is the effect from polarization. The kinematic effect is from the $(1 - \beta_t \cos\theta_{t\ell})^3$ factor in the denominator of Eqs. (7) and (8), which gives rise to peaking for large $\cos\theta_{t\ell}$. Also these anomalous couplings, which include momentum dependence, further give rise to enhancement or suppression in the top-boost depending on the sign of the couplings. Thus, for these couplings, there is enhancement or suppression of the peak in the azimuthal distribution near $\phi_\ell = 0$ and $\phi_\ell = 2\pi$.

Since the couplings Ref_{2R} and $\text{Re}\rho_2$ contribute significantly at the linear order to the production density matrices $\rho(\lambda, \lambda')$, the azimuthal distributions for Ref_{2R} and $\text{Re}\rho_2$ are quite distinct from the SM at $\phi_\ell = 0, 2\pi$. On the other hand, for the coupling $\text{Im}\rho_3$, the distribution almost overlaps with the SM curve, because its contribution at the linear order to the $\rho(\lambda, \lambda')$ is quite small.

3.4 Azimuthal Asymmetry

As we see from Fig. 9 that the curves are well separated at the peaks for the chosen values of the anomalous Wtb and ttg couplings and are also well separated from the curve for the SM. An asymmetry can be defined for the lepton to quantify these differences in the distributions as

$$A_\phi = \frac{\sigma(\cos\phi_\ell > 0) - \sigma(\cos\phi_\ell < 0)}{\sigma(\cos\phi_\ell > 0) + \sigma(\cos\phi_\ell < 0)}, \quad (13)$$

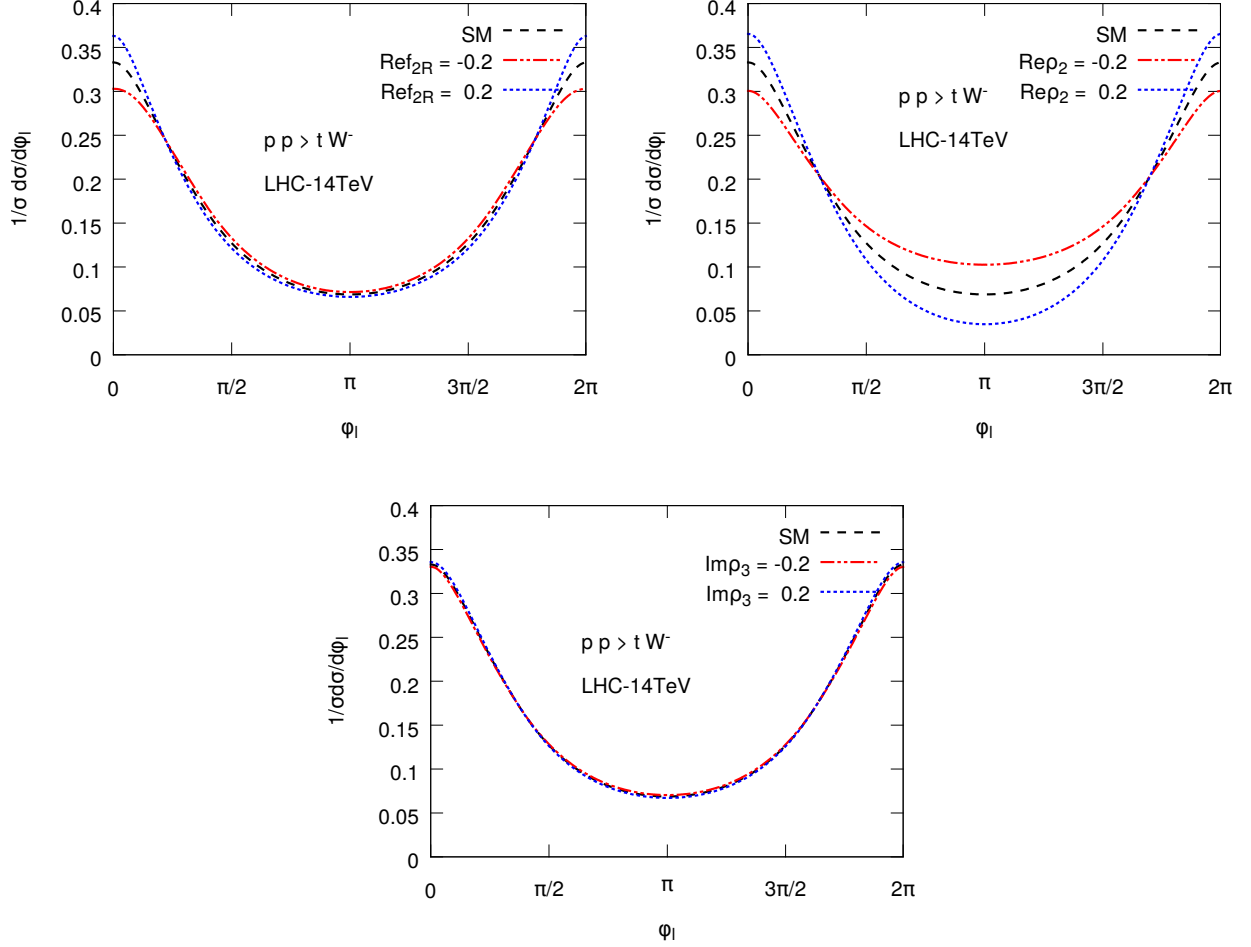


Figure 9: The normalized azimuthal distribution of the charged lepton in associated- Wt single-top production at the LHC14 for anomalous couplings Ref_{2R} , $\text{Re}\rho_2$ and $\text{Im}\rho_3$. The contributions of anomalous couplings are included up to linear order. Also shown in each case is the distribution for the SM.

where the denominator is the total cross section. This azimuthal asymmetry is in fact the “left-right asymmetry” of the charged lepton at the LHC defined with respect to the beam direction, with the right hemisphere defined as that in which the top momentum lies, and the left one being the opposite one. In Fig. 10 we show the plots of A_ϕ at LHC8 and LHC14 as a function of the couplings Ref_{2R} , $\text{Re}\rho_2$ and $\text{Im}\rho_3$ including their contributions up to the linear order. In Fig. 11 plots of A_ϕ are shown including the full contributions of the anomalous couplings at LHC8 and LHC14. The rapidity and transverse momentum acceptance cuts on the decay lepton that we have used to obtain all the distributions and asymmetries are $|\eta| < 2.5$, $p_T^\ell > 20$ GeV.

From Fig. 9, we see that the azimuthal distribution of the decay charged lepton is more sensitive to Ref_{2R} , $\text{Re}\rho_2$ than to $\text{Im}\rho_3$. Hence, we expect that the azimuthal asymmetry we construct in Eq. (13) would be a sensitive probe of Ref_{2R} and $\text{Re}\rho_2$. This fact can indeed be seen from Figs. 10, where the straight lines for $\text{Re}\rho_2$ and Ref_{2R} are steeper than for $\text{Im}\rho_3$

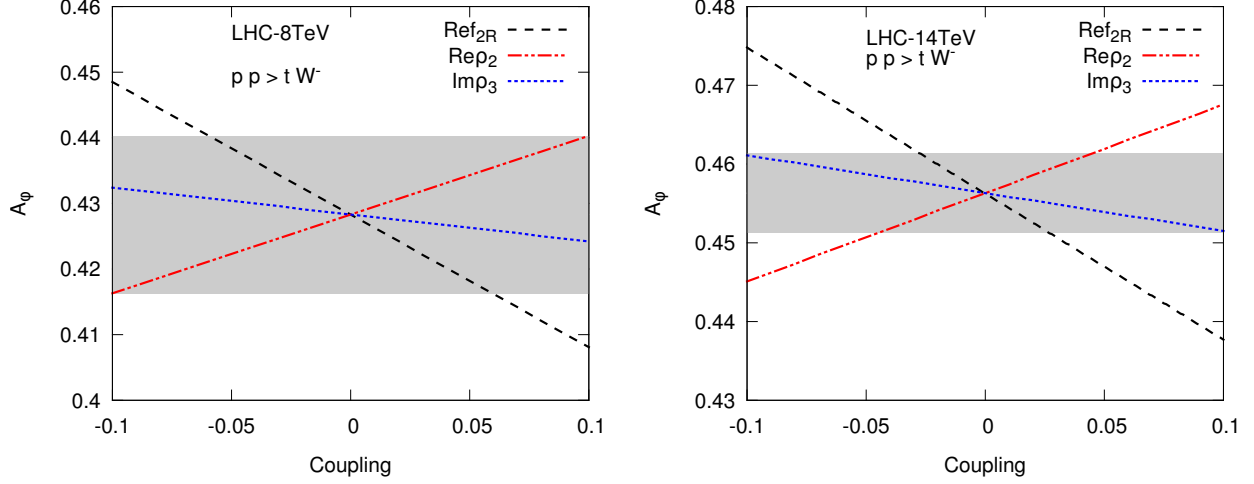


Figure 10: The azimuthal asymmetry of the charged lepton in associated- Wt single-top production at the LHC8 (left) and LHC14 (right) for different anomalous and Wtb and ttg couplings.

implying a more significant contribution from the former. The reason we get straight lines for individual contributions to the asymmetry is that we are working in a linear approximation for the anomalous couplings.

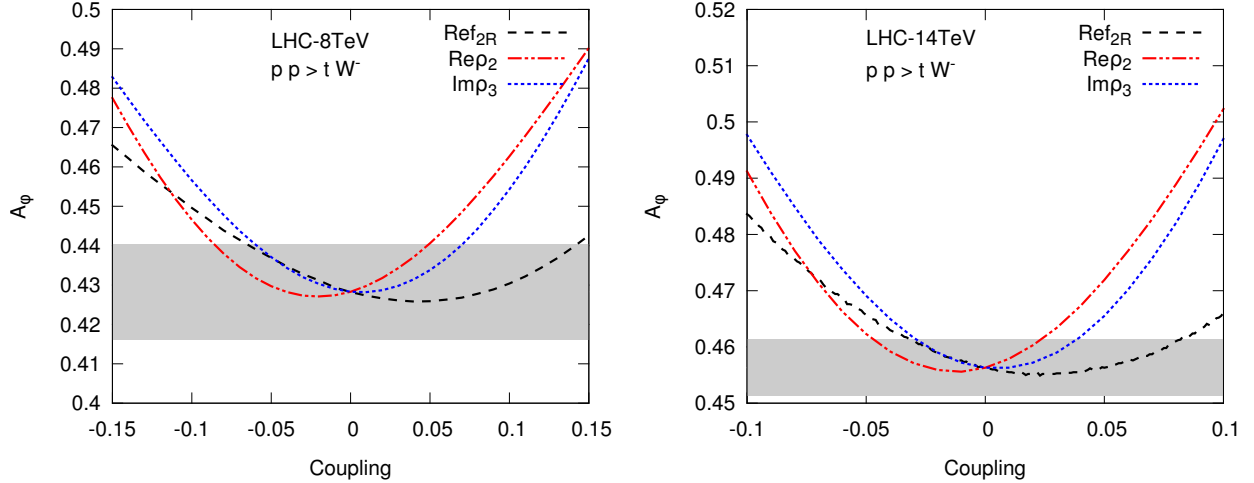


Figure 11: The azimuthal asymmetry of the charged lepton in associated- Wt single-top production at the LHC8 (left) and LHC14 (right) for different anomalous and Wtb and ttg couplings.

From Fig. 11, we find that the contributions of the couplings $Re\rho_2$ and $Im\rho_3$ are quite significant for relatively large values (~ 0.1) of the anomalous couplings and the linear approximations on these couplings are only valid in the range $[-0.02 : 0.02]$. Beyond this range, quadratic contributions from these couplings also become quite significant. A_ϕ is more sensitive to negative values of Ref_{2R} , whereas for $Re\rho_2$ it is more sensitive to positive values of the anomalous coupling. On the other hand, A_ϕ is almost symmetric around $Im\rho_3 = 0$, signifying that there is

only a very small contribution at linear order and it is equally sensitive to positive and negative values of the coupling. The reason behind is that the linear contributions from the coupling $\text{Im}\rho_3$ in the numerator and denominator have same sign and this tends to cancel the effect in the asymmetry. The grey bands in Figs. 10 and 11 denote the statistical uncertainty in the measurement of the asymmetry, which has been evaluated using the Eq. (14). For LHC8 and LHC14, integrated luminosities of 20 fb^{-1} and 30 fb^{-1} respectively have been used to evaluate the statistical uncertainties in the measurement of the observables.

4 Sensitivity analysis for anomalous tbW and ttg couplings

We now study the sensitivities of the observables discussed in the previous sections to the anomalous tbW and ttg couplings at the LHC, running at two cm of energies viz., 8 TeV and 14 TeV, with integrated luminosities 20 fb^{-1} and 30 fb^{-1} , respectively. To obtain the 1σ limit on the anomalous tbW and ttg couplings from a measurement of an observable, we find those values of the couplings for which observable deviates by 1σ from its SM value. The statistical uncertainty σ_i in the measurement of any generic asymmetry \mathcal{A}_i is given by

$$\sigma_i = \sqrt{\frac{1 - (\mathcal{A}_i^{SM})^2}{\mathcal{N}\epsilon}}, \quad (14)$$

where \mathcal{A}_i^{SM} is the asymmetry predicted in the SM, \mathcal{N} is the total number of events predicted in the SM and ϵ is the efficiency of the signal after applying all the acceptance and selection cuts to separate the signal from the background. We determine the efficiency to be approximately 0.1 by making use of Table 1 of [31] and also Table 1 of [32], where they search for Wt using leptonic decays of both the top and W . For the searches with hadronic decays of the W and semileptonic decay of the top, which is pertinent to our analysis, Ref. [33] indicates somewhat better efficiency than 0.1 for each channel. Thus, we are being somewhat conservative as we take $\epsilon = 0.1$. We apply this to the top polarization, top polar asymmetry and azimuthal asymmetry which we have discussed. In case of top polarization, the limits are obtained on the assumption that the polarization can be measured with only leptonic decays and thus only the semi-leptonic cross section has been used to calculate the statistical uncertainty.

The 1σ limits on $\text{Re}\rho_2$, $\text{Re}\rho_3$ and $\text{Im}\rho_3$ are given in Table 1 and 2 for LHC8 and LHC14, respectively, where we assume only one anomalous coupling to be non-zero at a time. We have also assumed measurements on a tW^- final state. Including the $\bar{t}W^+$ final state will improve the limits by a factor of $\sqrt{2}$. In case of the lepton distributions, we take into account only one leptonic channel. Again, including other leptonic decays of the top would improve the limits further. The limits corresponding to a linear approximation in the couplings are denoted by the label “lin. approx.”. Note that quadratic dependence is on $|\rho_2|^2$ and $|\rho_3|^2$, not on $\text{Re}\rho_2$ and $\text{Im}\rho_3$. Thus the limits obtained from the quadratic expressions assume that $\text{Im}\rho_2$ and $\text{Re}\rho_3$ are zero. Apart from the 1σ limits shown in Table 1, which correspond to intervals which include zero value of the

	8 TeV		
Observable	Ref _{2R}	Re ρ_2	Im ρ_3
P_t	$[-0.030, 0.032]$	$[-0.028, 0.019]$	$[-0.038, 0.065]$
P_t (lin. approx.)	$[-0.030, 0.030]$	$[-0.022, 0.022]$	$[-0.088, 0.088]$
A_ϕ	$[-0.060, 0.140]$	$[-0.080, 0.050]$	$[-0.055, 0.070]$
A_ϕ (lin. approx.)	$[-0.065, 0.065]$	$[-0.100, 0.100]$	$[-0.295, 0.295]$

Table 1: Individual limits on anomalous couplings Ref_{2R}, Re ρ_2 and Im ρ_3 which may be obtained by the measurement of the observables shown in the first column of the table at 8 TeV with integrated luminosities of 20 fb⁻¹.

coupling, there are other disjoint intervals which could be ruled out if no deviation from the SM is observed for P_t and A_ϕ . This is apparent from Fig. 7. The additional allowed intervals for Ref_{2R} and Re ρ_2 from P_t measurement are $[0.158, 0.205]$ and $[-0.80, -0.65]$ for LHC14, respectively¹. It is seen that the top polarization, P_t , and azimuthal asymmetry, A_ϕ , of the charged lepton are more sensitive to negative values of the anomalous couplings Ref_{2R} and positive values of Re ρ_2 . In Fig. 12 we show projected individual limits (taking only one coupling nonzero at a time) on the anomalous couplings Ref_{2R}, Re ρ_2 and Im ρ_3 , obtained from the measurement of A_ϕ at the LHC14 as a function of integrated luminosity. With 100 fb⁻¹ of integrated luminosity, the projected limits on Ref_{2R}, Re ρ_2 and Im ρ_3 are $[-0.006, 0.006]$, $[-0.005, 0.005]$ and $[-0.015, 0.015]$ respectively.

	14 TeV		
Observable	Ref _{2R}	Re ρ_2	Im ρ_3
P_t	$[-0.010, 0.010]$	$[-0.009, 0.009]$	$[-0.020, 0.035]$
P_t (lin. approx.)	$[-0.010, 0.010]$	$[-0.009, 0.009]$	$[-0.030, 0.030]$
A_ϕ	$[-0.031, 0.081]$	$[-0.045, 0.020]$	$[-0.030, 0.040]$
A_ϕ (lin. approx.)	$[-0.060, 0.060]$	$[-0.045, 0.045]$	$[-0.100, 0.100]$

Table 2: Individual limits on anomalous couplings Ref_{2R}, Re ρ_2 and Im ρ_3 which may be obtained by the measurement of the observables shown in the first column of the table at 14 TeV with integrated luminosities of 30 fb⁻¹.

We also obtain simultaneous limits (taking two couplings out of Ref_{2R}, Re ρ_2 and Im ρ_3 non-zero simultaneously) on these anomalous couplings that may be obtained by the measurements of asymmetries. For this, we perform a χ^2 analysis to fit all the observables to within $f\sigma$ of statistical errors in the measurement of the observable. We define the following χ^2 function

$$\chi^2 = \sum_{i=1}^n \left(\frac{P_i - O_i}{\sigma_i} \right)^2, \quad (15)$$

¹[a, b] denotes the allowed values of the coupling f at the 1 σ level, satisfying $a < f < b$.

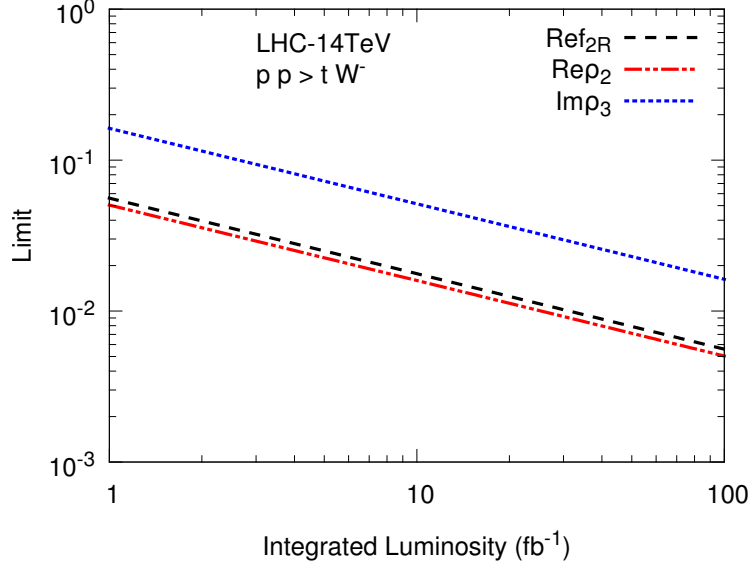


Figure 12: The 1σ limit on the anomalous couplings from the measurement of azimuthal asymmetry A_ϕ as a function of integrated luminosity at LHC14.

where the sum runs over the n observables measured and f is the degree of the confidence interval. The P_i 's are the values of the observables obtained by taking two couplings out of Ref_{2R} , $\text{Re}\rho_2$ and $\text{Im}\rho_3$ non-zero simultaneously and the O_i 's are the values of the observables obtained in the SM. The σ_i 's are the statistical fluctuations in the measurement of the observables, given in Eq. (14).

In Fig. 13, we show the 1σ , 2σ and 3σ regions in $\text{Ref}_{2R} - \text{Re}\rho_2$ plane, $\text{Ref}_{2R} - \text{Im}\rho_3$ plane and $\text{Re}\rho_2 - \text{Im}\rho_3$ plane allowed by the measurement of the asymmetry A_ϕ . From the plots shown in Fig. 13, we find that the strongest simultaneous limits are $[-0.03, 0.08]$ on Ref_{2R} , $[-0.05, 0.02]$ on $\text{Re}\rho_2$ and $[-0.03, 0.03]$ on $\text{Im}\rho_3$, at the 1σ level.

We now compare our results with those of other relevant works on the determination of anomalous ttg couplings at the LHC. Ref. [53] studies the top quark compositeness and put a stringent limit of $|0.01|$ on top-CMDM coupling using top-pair production cross section and spin correlations at LHC7 and LHC8. In Ref. [14], the authors used top polarization asymmetry and azimuthal asymmetry in top pair production to probe $\text{Re}\rho_2$ and $\text{Im}\rho_3$ at the Tevatron and LHC. Their conclusion was that top polarization P_t is only sensitive to $\text{Im}\rho_3$ and not $\text{Re}\rho_2$. On the other hand, in the Wt -mode of single-top production, we find opposite results. Here P_t is more sensitive to $\text{Re}\rho_2$ than to $\text{Im}\rho_3$. We also find that the limits which we obtained on anomalous couplings are about an order of magnitude smaller than those obtained in Ref [14] for top pair production from the observables considered in this work. In Ref. [43] Rizzo studied anomalous ttg couplings in single-top production at the Tevatron and at the LHC and concluded that the limits from this channel are about one order of magnitude smaller than those from the pair production processes.

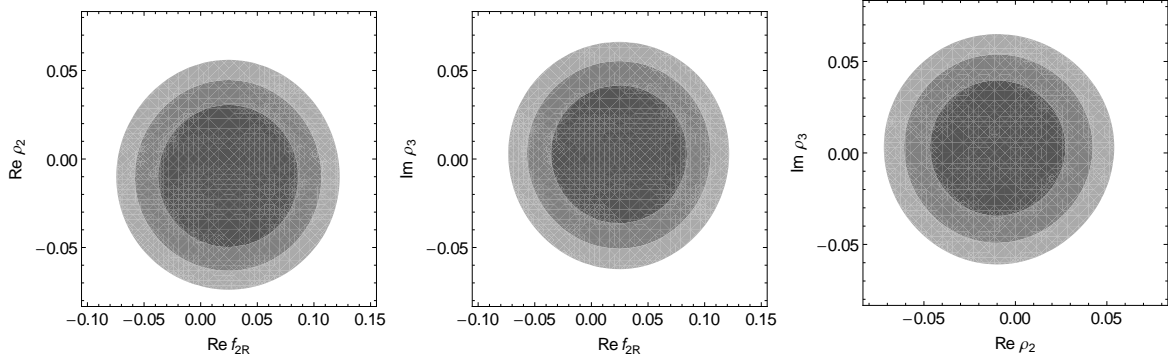


Figure 13: The 1σ (central region), 2σ (middle region) and 3σ (outer region) CL regions in the $\text{Re}f_{2R}$ - $\text{Re}\rho_2$ plane (left), $\text{Re}f_{2R}$ - $\text{Im}\rho_3$ plane (center) and $\text{Re}\rho_2$ - $\text{Im}\rho_3$ plane (right) allowed by the measurement of the azimuthal asymmetry at the LHC14. The χ^2 value for the 1σ , 2σ and 3σ CL intervals are 2.30, 6.18 and 11.83 respectively, for two parameter fit.

5 Conclusions

We have investigated the sensitivity of the LHC8 and LHC14 to the anomalous ttg couplings in Wt mode of single-top production followed by semileptonic decay of the top. We derived analytical expressions for the spin density matrix for single-top-quark production, including the contributions of both real and imaginary parts of the anomalous ttg couplings. We find that only $\text{Re}\rho_2$ and $\text{Im}\rho_3$ give significant contributions to the spin density matrix at linear order. It may be noted that $\text{Im}\rho_2$ and $\text{Re}\rho_3$ do not appear in the observables we consider. This may be understood from the CPT theorem which implies that our observables, being even under naive time reversal T , can only get a non vanishing contribution from dispersive parts of CP-even form factors (in this case $\text{Re}\rho_2$) and from absorptive parts (in this case $\text{Im}\rho_3$) of CP-odd form factors.

Since top polarization can be measured only through the differential distribution of its decay products, we also study the angular distributions of the charged lepton coming from the decay of the top. We mainly focus on charged-lepton distribution for three reasons : a) charged-lepton momenta are very accurately measured at the LHC, b) they have the best spin analyzing power and c) their angular distributions have been shown to be independent of any new physics in top decay. We find that the polar-angle distribution is not very sensitive to the anomalous couplings. On the other hand, the normalized azimuthal distribution is found to be sensitive to the anomalous couplings. The azimuthal distribution peaks close to $\phi = 0$ and $\phi = 2\pi$ and the values at the peaks are quite sensitive to the magnitude and the sign of the anomalous couplings. In order to quantify this difference and to be statistically more sensitive, we construct an integrated azimuthal asymmetry from the azimuthal distribution of charged lepton.

Our observables, in this work, are constructed from one of the two conjugate single-top processes possible, viz., tW^- in the final state. Under a CP transformation, since helicity changes sign, a positive helicity top quark transforms to a negative helicity top anti-quark. If CP is conserved, the spin density matrix, $\bar{\sigma}$, for the top anti-quark in the $\bar{t}W^+$ production process would be obtained from that of the top quark in the tW^- production process by reversing the sign

of helicities i.e., $\bar{\sigma}^{\pm,\pm} = \sigma^{\mp,\mp}$ and $\sigma^{\pm,\mp} = \sigma^{\mp,\pm}$. However, since $\text{Im}\rho_3$ is CP odd, the contribution of $\text{Im}\rho_3$ in the $\bar{\sigma}$ would change sign. Also, because of CPT transformation properties, the signs of $\text{Im}\rho_2$ and $\text{Re}\rho_3$ in the $\bar{\sigma}^{\pm,\mp}$ also change. If we combine observables from tW^- production as well as $\bar{t}W^+$ production, it is possible to construct observables with definite CP properties enabling us to separate contributions from ρ_2 and ρ_3 , which have opposite CP transformation properties. The simplest of these would be the sum (difference) of the tW^- and tW^+ production cross sections which would be CP even (odd) and the sum (difference) of t and \bar{t} polarizations in the two processes, which would be CP odd (even). With the availability in future of large event samples in the high-luminosity version of the experiment, it would be possible to separately constrain CP-even and CP-odd couplings.

Our proposal provides an alternative other than top-pair production to look for top CMDM and CEDM in single-top production. The Wt mode is also significant in the probe of these couplings because it does not get any contributions from other new physics like new resonances, exotic quarks or scalars which could contaminate other single-top production modes and $t\bar{t}$ -production process.

We also note that the production cross section at 13 TeV is about 15% lower than the 14 TeV cross section, while the asymmetry and top polarization are not very sensitive to the cm energy of the LHC. The latter change by less than a percent. Thus, the sensitivities would only be affected by the 15% reduction in the total number of events at 13 TeV relative to 14 TeV LHC for the same amount of integrated luminosity. This would amount to a reduction in sensitivity to the couplings of about 7%.

In conclusion, we have shown that top polarization, and subsequent decay-lepton distributions can be used to obtain fairly stringent limits on chromomagnetic and chromoelectric top couplings from the existing 8 TeV run of the LHC. The limits could be improved by the future runs of the LHC at 14 TeV.

Our results would be somewhat worsened by the inclusion of realistic detection efficiencies for the b jet and for the detection of the W . On the other hand, inclusion of the $\bar{t}W^+$ final state, as well as additional leptonic channels in top decay would contribute to improving on our estimates of the limits. A more complete analysis including detector simulation would be worthwhile to carry out.

Acknowledgements

SDR acknowledges support from the Department of Science and Technology, India, under the J.C. Bose National Fellowship programme, Grant No. SR/SB/JCB-42/2009. This work was supported by the Australian Research Council through the ARC Centre of Excellence in Particle Physics at the Terascale (CE110001004) and grant FL0992247

Appendix: Spin-density matrix elements of top quark in tW production including anomalous top-gluon couplings

In the appendix, we give the spin density matrix elements for the tW single-top production process. We include the contributions of top CMDM and CEDM up to the linear order. The diagonal elements of the spin density matrix can be written as

$$\rho^{\pm\pm} = \rho_{s,SM}^{\pm\pm} + \rho_{t,SM}^{\pm\pm} + \rho_{st,SM}^{\pm\pm} + \rho_{t,\text{Re}\rho_2}^{\pm\pm} + \rho_{st,\text{Re}\rho_2}^{\pm\pm} + \rho_{t,\text{Im}\rho_3}^{\pm\pm} + \rho_{st,\text{Im}\rho_3}^{\pm\pm} \quad (16)$$

where s , t and st in the subscript denote the contribution from s -channel, t -channel and interference between s and t channels respectively.

$$\begin{aligned} \rho_{s,SM}^{\pm\pm} &= \frac{g^2 g_s^2}{24 \hat{s}} \frac{1}{m_W^2} \left[(\hat{t} + \hat{u} + m_W^2) (\hat{t} - m_W^2) + \hat{s} m_W^2 \right. \\ &\quad \left. \pm 2m_t \{ \mathcal{S}_{gn} (\hat{t} - 2m_W^2) + \mathcal{S}_{bn} (\hat{t} - m_W^2) \} \right] \end{aligned} \quad (17)$$

$$\begin{aligned} \rho_{t,SM}^{\pm\pm} &= \frac{g^2 g_s^2}{24 (\hat{t} - m_t^2)^2} \frac{1}{m_t^2 m_W^2} \left[m_t^2 (\hat{u} - m_W^2) (m_t^2 - 4m_W^2 - 4\hat{u}) + \hat{u}^2 (m_t^2 - \hat{t}) - \hat{s} \hat{u} m_t^2 \right. \\ &\quad + 2\hat{s} m_W^2 (m_t^2 - \hat{u}) \pm 2m_t \mathcal{S}_{gn} (m_t^2 - 2m_W^2) (m_W^2 - \hat{u}) \\ &\quad \left. \pm 2m_t \mathcal{S}_{bn} (2m_W^2 - \hat{u}) (m_t^2 + \hat{u}) \right] \end{aligned} \quad (18)$$

$$\begin{aligned} \rho_{st,SM}^{\pm\pm} &= \frac{g^2 g_s^2}{24 (\hat{t} - m_t^2)} \frac{2}{m_W^2} \left[\hat{s} \left\{ (m_t^2 - \hat{t}) (m_t^2 + 2m_W^2) + \hat{u} m_t^2 + m_t^4 + \hat{t} \hat{u} \right\} \right. \\ &\quad + (-2m_t^2 + \hat{u} + \hat{t}) (m_t^2 - \hat{t}) (m_t^2 + 2m_W^2) \pm m_t \mathcal{S}_{gn} \left\{ (-2m_t^2 + 2m_W^2 + \hat{u}) (m_t^2 - \hat{t}) + 2m_t^2 \hat{s} \right\} \\ &\quad \left. \pm m_t \mathcal{S}_{bn} \left\{ -2(\hat{u} - m_W^2) (m_t^2 - 2m_W^2) + (2m_W^2 - \hat{u}) (m_t^2 - \hat{u}) + 2\hat{s} \hat{u} \right\} \right] \end{aligned} \quad (19)$$

$$\begin{aligned} \rho_{t,\text{Re}\rho_2}^{\pm\pm} &= \frac{g^2 g_s^2}{24 (\hat{t} - m_t^2)^2} \frac{\text{Re}\rho_2}{m_t^2 m_W^2} \left[3m_t^2 \left[(m_t^2 - \hat{u})^2 (m_t^2 - \hat{t}) + \hat{s} (m_t^2 - \hat{u}) (2m_W^2 - m_t) \right] \right. \\ &\quad \pm m_t \left\{ \mathcal{S}_{gn} \left[(2m_W^2 - 2m_t^2 - \hat{u}) (m_t^2 - \hat{u}) (m_t^2 - \hat{t}) \right] \right. \\ &\quad \left. \left. + 2\hat{s} m_t^2 (m_t^2 - 4m_W^2 + \hat{u}) \right] \pm \mathcal{S}_{bn} \left[(\hat{u} - 2m_W^2) (m_t^2 - \hat{u})^2 \right] \right\} \end{aligned} \quad (20)$$

$$\begin{aligned} \rho_{st,\text{Re}\rho_2}^{\pm\pm} &= \frac{g^2 g_s^2}{24 (\hat{t} - m_t^2)} \frac{\text{Re}\rho_2}{m_t m_W^2} \left[m_t \hat{s} \left\{ (\hat{t} - m_W^2) (m_t^2 - 2m_W^2) - 2m_W^2 m_t^2 + 3\hat{u} \hat{t} - m_t^2 \hat{t} \right\} \right. \\ &\quad \pm 2 \left\{ (m_t^2 - \hat{t}) (m_t^2 - 2m_W^2) - 2m_W^2 (m_t^2 - \hat{u}) \right\} \left\{ (m_t^2 - \hat{t}) \mathcal{S}_{gn} - (m_t^2 - \hat{u}) \mathcal{S}_{bn} \right\} \\ &\quad \pm \hat{s} \left\{ (m_t^2 - \hat{u}) \mathcal{S}_{bn} - (m_t^2 - \hat{t}) \mathcal{S}_{gn} \right\} (m_t^2 - 2m_W^2) \pm \hat{s} \mathcal{S}_{gn} (3m_t^2 m_W^2 + \hat{t} \hat{u} - m_t^2 \hat{s}) \\ &\quad \left. \pm \hat{s} \mathcal{S}_{bn} \{ m_t^4 - u^2 - 4m_t^2 (2m_W^2 - \hat{u}) \} \right] \end{aligned} \quad (21)$$

$$\begin{aligned}
\rho_{t,\text{Im}\rho_3}^{\pm\pm} &= \frac{g^2 g_s^2}{24 (\hat{t} - m_t^2)^2} \frac{\text{Im}\rho_3}{m_t^2 m_W^2} \left[m_t^2 \left\{ (m_t^2 - \hat{u}) \left[(m_t^2 - \hat{t})(4m_W^2 - 3m_t^2 + \hat{u}) + \hat{s}(m_t^2 - 2m_W^2 - 2\hat{u}) \right] \right. \right. \\
&+ 2\hat{s} m_t^2 (m_t^2 - 2m_W^2) \left. \right\} \pm m_t \mathcal{S}_{gn} \left\{ -2\hat{s} m_t^2 (m_t^2 - 3\hat{u} - 4m_W^2) + (m_t^2 - \hat{t}) \right. \\
&\times \left. \left. \left[(2m_t^2 - 6m_W^2 - \hat{u})(m_t^2 - \hat{u}) - 4\hat{u}(2m_W^2 + m_t^2) \right] \right\} \pm m_t \mathcal{S}_{bn} (\hat{u} - 2m_W^2)(m_t^2 - \hat{u})^2 \right]
\end{aligned} \tag{22}$$

$$\begin{aligned}
\rho_{st,\text{Im}\rho_3}^{\pm\pm} &= \frac{g^2 g_s^2}{24 (\hat{t} - m_t^2)^2} \frac{\text{Im}\rho_3}{m_t m_W^2} \left[m_t \hat{s} \left\{ m_W^2 (m_t^2 + 2m_W^2) - 6m_W^2 m_t^2 + 2\hat{u} m_t^2 + (2m_W^2 - \hat{u})\hat{t} - 2\hat{s}\hat{u} \right\} \right. \\
&+ 2 \mathcal{S}_{gn} \left\{ (\hat{t} - m_t^2)(m_t^2 + 2m_W^2) + 2 m_W^2 (\hat{u} - m_t^2) + \hat{s}(2m_t^2 + m_W^2) \right\} (m_t^2 - \hat{t}) \\
&+ \hat{s} \mathcal{S}_{gn} (\{3\hat{u} - 2\hat{s}\} m_t^2 + \hat{t}\hat{u}) + \mathcal{S}_{bn} \left\{ (-2m_t^2 - 2m_W^2 + \hat{u})\hat{s} + 2(m_t^2 - \hat{t})(m_t^2 + 2m_W^2) \right. \\
&+ \left. \left. 4m_W^2 (m_t^2 - \hat{u}) \right\} (m_t^2 - \hat{u}) \right]
\end{aligned} \tag{23}$$

where \hat{s} , \hat{t} and \hat{u} are the Mandelstam variables in the parton cm frame, $\mathcal{S}_{bn} = p_b \cdot n_3$ and $\mathcal{S}_{gn} = p_g \cdot n_3$. n_3 is the longitudinal spin vector of the top quark, whose components are given by

$$n_3 \equiv \frac{E_t}{m_t} (\beta_t, \sin \theta_t, 0, \cos \theta_t). \tag{24}$$

The off-diagonal elements with helicity combination $\pm\mp$ corresponding to each of the terms on the right-hand side of Eq. (16) are given by n_3 dependent terms of the diagonal elements for the corresponding term in Eqs. (17)-(23), with the vector n_3 replaced by $\frac{1}{2}(n_1 \mp i n_2)$, where

$$n_1 \equiv (0, \cos \theta_t, 0, -\sin \theta_t) \tag{25}$$

and

$$n_2 \equiv (0, 0, 1, 0). \tag{26}$$

Moreover there are additional contributions to the spin density matrix elements for helicity combination $\pm\mp$ which come from couplings $\text{Im}\rho_2$ and $\text{Re}\rho_3$ and are given by

$$\rho_{t,\text{Im}\rho_2}^{\pm\mp} = \frac{g^2 g_s^2}{24 (\hat{t} - m_t^2)^2} \frac{\text{Im}\rho_2}{m_t m_W^2} \epsilon_{\mu\nu\rho\sigma} p_t^\mu p_b^\nu p_g^\rho (n_1^\sigma \mp i n_2^\sigma) \left[(2m_W^2 - \hat{u})(m_t^2 - u) \right] \tag{27}$$

$$\rho_{t,\text{Re}\rho_3}^{\pm\mp} = \frac{g^2 g_s^2}{24 (\hat{t} - m_t^2)^2} \frac{\text{Re}\rho_3}{m_t m_W^2} \epsilon_{\mu\nu\rho\sigma} p_t^\mu p_b^\nu p_g^\rho (n_1^\sigma \mp i n_2^\sigma) \left[(2m_W^2 - \hat{u})(3m_t^2 + u) \right] \tag{28}$$

$$\begin{aligned}\rho_{st, \text{Im}\rho_2}^{\pm\mp} &= \frac{g^2 g_s^2}{24 (\hat{t} - m_t^2)} \frac{\text{Im}\rho_2}{m_t m_W^2} \epsilon_{\mu\nu\rho\sigma} p_t^\mu p_b^\nu p_g^\rho (n_1^\sigma \mp i n_2^\sigma) \left[(m_t^2 + 2m_W^2)(-2m_t^2 + 2\hat{t} + \hat{s}) \right. \\ &\quad \left. + (\hat{s} - 4m_W^2)(m_t^2 - \hat{u}) \right]\end{aligned}\quad (29)$$

$$\begin{aligned}\rho_{st, \text{Re}\rho_3}^{\pm\mp} &= \frac{g^2 g_s^2}{24 (\hat{t} - m_t^2)} \frac{\text{Re}\rho_3}{m_t m_W^2} \epsilon_{\mu\nu\rho\sigma} p_t^\mu p_b^\nu p_g^\rho (n_1^\sigma \mp i n_2^\sigma) \left[(m_t^2 - 2m_W^2)(-2m_t^2 + 2\hat{t} + \hat{s}) \right. \\ &\quad \left. + 4m_W^2(m_t^2 - \hat{u}) + (m_t^2 + \hat{u})\hat{s} \right]\end{aligned}\quad (30)$$

References

- [1] [Tevatron Electroweak Working Group and CDF and D0 Collaborations], arXiv:1107.5255 [hep-ex].
- [2] G. Aad *et al.* [ATLAS Collaboration], Phys. Rev. Lett. **108**, 212001 (2012) [arXiv:1203.4081 [hep-ex]].
- [3] CMS Collaoration, CMS Physics Analysis Summary, CMS-PAS-TOP-12-004.
- [4] ATLAS Collaboration, Atlas note, ATLAS-CONF-2012-133; CMS Collaboration, CMS Physics Analysis Summary, CMS-PAS-TOP-12-016.
- [5] W. Bernreuther, J. Phys. G **35**, 083001 (2008) [arXiv:0805.1333 [hep-ph]].
- [6] W. Bernreuther and P. Uwer, Nucl. Part. Phys. Proc. **261-262**, 414.
- [7] W. Bernreuther and Z. G. Si, Phys. Lett. B **725**, 115 (2013) [Phys. Lett. B **744**, 413 (2015)] [arXiv:1305.2066 [hep-ph]].
- [8] R. M. Godbole, K. Rao, S. D. Rindani and R. K. Singh, JHEP **1011**, 144 (2010) [arXiv:1010.1458 [hep-ph]].
- [9] K. Huitu, S. Kumar Rai, K. Rao, S. D. Rindani and P. Sharma, JHEP **1104**, 026 (2011) [arXiv:1012.0527 [hep-ph]].
- [10] R. M. Godbole, L. Hartgring, I. Niessen and C. D. White, JHEP **1201**, 011 (2012) [arXiv:1111.0759 [hep-ph]].
- [11] S. D. Rindani and P. Sharma, JHEP **1111**, 082 (2011) [arXiv:1107.2597 [hep-ph]].
- [12] A. Prasath, R. M. Godbole and S. D. Rindani, arXiv:1405.1264 [hep-ph]; R. M. Godbole, S. D. Rindani and R. K. Singh, Phys. Rev. D **67**, 095009 (2003) [Erratum-ibid. D **71**, 039902 (2005)] [hep-ph/0211136].

- [13] S. D. Rindani and P. Sharma, Phys. Lett. B **712**, 413 (2012) [arXiv:1108.4165 [hep-ph]].
- [14] S. S. Biswal, S. D. Rindani and P. Sharma, Phys. Rev. D **88**, 074018 (2013) [arXiv:1211.4075 [hep-ph]].
- [15] S. D. Rindani, R. Santos and P. Sharma, JHEP **1311**, 188 (2013) [arXiv:1307.1158].
- [16] D. Choudhury, R. M. Godbole, S. D. Rindani and P. Saha, Phys. Rev. D **84**, 014023 (2011) [arXiv:1012.4750 [hep-ph]]; D. -W. Jung, P. Ko and J. S. Lee, Phys. Lett. B **701**, 248 (2011) [arXiv:1011.5976 [hep-ph]]; R. M. Godbole, G. Mendiratta and S. Rindani, arXiv:1506.07486 [hep-ph]; J. Cao, K. Hikasa, L. Wang, L. Wu and J. M. Yang, Phys. Rev. D **85**, 014025 (2012) [arXiv:1109.6543 [hep-ph]].
- [17] A. Heinson, A. S. Belyaev, E. E. Boos, Phys. Rev. **D56**, 3114-3128 (1997) [hep-ph/9612424].
- [18] T. Stelzer, Z. Sullivan and S. Willenbrock, Phys. Rev. D **58**, 094021 (1998) [arXiv:hep-ph/9807340].
- [19] A. S. Belyaev, E. E. Boos and L. V. Dudko, Phys. Rev. D **59**, 075001 (1999) [arXiv:hep-ph/9806332].
- [20] E. Boos, L. Dudko and T. Ohl, Eur. Phys. J. C **11**, 473 (1999) [arXiv:hep-ph/9903215].
- [21] T. M. P. Tait, Phys. Rev. D **61**, 034001 (2000) [arXiv:hep-ph/9909352].
- [22] D. Espriu and J. Manzano, Phys. Rev. D **65**, 073005 (2002) [arXiv:hep-ph/0107112].
- [23] D. Espriu and J. Manzano, Phys. Rev. D **66**, 114009 (2002) [arXiv:hep-ph/0209030].
- [24] T. M. P. Tait and C. P. P. Yuan, Phys. Rev. D **63**, 014018 (2000) [arXiv:hep-ph/0007298].
- [25] C. D. White, S. Frixione, E. Laenen, F. Maltoni, JHEP **0911**, 074 (2009). [arXiv:0908.0631 [hep-ph]].
- [26] S. Frixione, E. Laenen, P. Motylinski, B. R. Webber, C. D. White, JHEP **0807**, 029 (2008). [arXiv:0805.3067 [hep-ph]].
- [27] S. Frixione, E. Laenen, P. Motylinski, B. R. Webber, JHEP **0603**, 092 (2006). [hep-ph/0512250].
- [28] S. Chatrchyan *et al.* [CMS Collaboration], Phys. Rev. Lett. **107**, 091802 (2011) [arXiv:1106.3052 [hep-ex]].
- [29] V. Khachatryan *et al.* [CMS Collaboration], JHEP **1406**, 090 (2014) [arXiv:1403.7366 [hep-ex]].
- [30] G. Aad *et al.* [ATLAS Collaboration], Phys. Rev. D **90**, no. 11, 112006 (2014) [arXiv:1406.7844 [hep-ex]].

- [31] G. Aad *et al.* [ATLAS Collaboration], Phys. Lett. B **716**, 142 (2012) [arXiv:1205.5764 [hep-ex]].
- [32] S. Chatrchyan *et al.* [CMS Collaboration], Phys. Rev. Lett. **112**, no. 23, 231802 (2014) [arXiv:1401.2942 [hep-ex]].
- [33] A. Lucotte, A. Llres, D. Chevallier, ATLAS note ATL-PHYS-PUB-2007-005.
- [34] ATLAS and CMS Collaborations, ATLAS-CONF-2014-052, CMS-PAS-TOP-14-009
- [35] CMS collab., CMS report CMS-PAS-TOP-13-001
- [36] R. Martinez, M. A. Perez and N. Poveda, Eur. Phys. J. C **53**, 221 (2008) [hep-ph/0701098].
- [37] E. P. Shabalin, Yad. Eiz., **28**, 151 (1978); **31**, 1665 (1980); [Sov. J. Nucl. Phys., **28**, 75 (1978)]; I. B. Khriplovich, Phys. Lett. B **173**, 193 (1986); Sov. J. Nucl. Phys. **44**, 659 (1986); YAFIA **44**, 1019 (1986); A. Czarnecki and B. Krause, Phys. Rev. Lett. **78**, 4339 (1997).
- [38] J. M. Yang and C. S. Li, Phys. Rev. D **54**, 4380 (1996) [hep-ph/9603442].
- [39] R. Martinez and J. A. Rodriguez, Phys. Rev. D **65**, 057301 (2002) [hep-ph/0109109].
- [40] R. Gaitan, E. A. Garces, J. H. M. de Oca and R. Martinez, arXiv:1505.04168 [hep-ph].
- [41] Q. -H. Cao, C. -R. Chen, F. Larios and C. -P. Yuan, Phys. Rev. D **79**, 015004 (2009) [arXiv:0801.2998 [hep-ph]]; L. Ding and C. -X. Yue, Commun. Theor. Phys. **50**, 441 (2008) [arXiv:0801.1880 [hep-ph]].
- [42] R. Martinez, M. A. Perez and O. A. Sampayo, Int. J. Mod. Phys. A **25**, 1061 (2010) [arXiv:0805.0371 [hep-ph]].
- [43] T. G. Rizzo, Phys. Rev. D **53**, 6218 (1996) [hep-ph/9506351].
- [44] S. Y. Ayazi, H. Hesari and M. M. Najafabadi, Phys. Lett. B **727**, 199 (2013) [arXiv:1307.1846 [hep-ph]].
- [45] M. Fabbrichesi, M. Pinamonti and A. Tonero, Eur. Phys. J. C **74**, no. 12, 3193 (2014) [arXiv:1406.5393 [hep-ph]].
- [46] D. Atwood, A. Kagan and T. G. Rizzo, Phys. Rev. D **52**, 6264 (1995) [hep-ph/9407408].
- [47] P. Haberl, O. Nachtmann and A. Wilch, Phys. Rev. D **53**, 4875 (1996) [hep-ph/9505409].
- [48] Z. Hioki and K. Ohkuma, Phys. Rev. D **83**, 114045 (2011) [arXiv:1104.1221 [hep-ph]]; arXiv:1206.2413 [hep-ph].
- [49] D. Choudhury and P. Saha, Pramana **77**, 1079 (2011) [arXiv:0911.5016 [hep-ph]].

- [50] Z. Hioki and K. Ohkuma, Eur. Phys. J. C **65**, 127 (2010) [arXiv:0910.3049 [hep-ph]]; Eur. Phys. J. C **71**, 1535 (2011) [arXiv:1011.2655 [hep-ph]].
- [51] H. Hesari and M. M. Najafabadi, arXiv:1207.0339 [hep-ph].
- [52] S. K. Gupta and G. Valencia, Phys. Rev. D **81**, 034013 (2010) [arXiv:0912.0707 [hep-ph]]; S. K. Gupta, A. S. Mete and G. Valencia, Phys. Rev. D **80**, 034013 (2009) [arXiv:0905.1074 [hep-ph]].
- [53] M. Fabbrichesi, M. Pinamonti and A. Tonero, Phys. Rev. D **89**, no. 7, 074028 (2014) [arXiv:1307.5750 [hep-ph]].
- [54] K. -m. Cheung, Phys. Rev. D **53**, 3604 (1996) [hep-ph/9511260].
- [55] K. -m. Cheung, Phys. Rev. D **55**, 4430 (1997) [hep-ph/9610368].
- [56] H. -Y. Zhou, Phys. Rev. D **58**, 114002 (1998) [hep-ph/9805358].
- [57] C. Englert, A. Freitas, M. Spira and P. M. Zerwas, arXiv:1210.2570 [hep-ph].
- [58] J. L. Hewett and T. G. Rizzo, Phys. Rev. D **49**, 319 (1994) [hep-ph/9305223].
- [59] R. Martinez and J. A. Rodriguez, Phys. Rev. D **55**, 3212 (1997) [hep-ph/9612438]; J. F. Kamenik, M. Papucci and A. Weiler, Phys. Rev. D **85**, 071501 (2012) [arXiv:1107.3143 [hep-ph]].
- [60] R. M. Godbole, S. D. Rindani and R. K. Singh, JHEP **0612**, 021 (2006) [hep-ph/0605100];
- [61] B. Grzadkowski and Z. Hioki, Phys. Lett. B **476**, 87 (2000) [hep-ph/9911505]; S. D. Rindani, Pramana **54**, 791 (2000) [hep-ph/0002006]; B. Grzadkowski and Z. Hioki, Phys. Lett. B **529**, 82 (2002) [hep-ph/0112361]; Phys. Lett. B **557**, 55 (2003) [hep-ph/0208079]; Z. Hioki, hep-ph/0210224.
- [62] J. A. M. Vermaseren, arXiv:math-ph/0010025.
- [63] J. Pumplin, A. Belyaev, J. Huston, D. Stump and W. K. Tung, JHEP **0602**, 032 (2006) [arXiv:hep-ph/0512167].